AIP | The Journal of Chemical Physics

NEXAFS spectroscopy and site-specific fragmentation of N-methylformamide, N,N-dimethylformamide, and N,N-dimethylacetamide

Peter Salén, Vasyl Yatsyna, Luca Schio, Raimund Feifel, Robert Richter, Michele Alagia, Stefano Stranges, and Vitali Zhaunerchyk

Citation: The Journal of Chemical Physics **144**, 244310 (2016); doi: 10.1063/1.4954704
View online: http://dx.doi.org/10.1063/1.4954704
View Table of Contents: http://scitation.aip.org/content/aip/journal/jcp/144/24?ver=pdfcov
Published by the AIP Publishing

NEXAFS spectroscopy and site-specific fragmentation of *N*-methylformamide, *N,N*-dimethylformamide, and *N,N*-dimethylacetamide

Peter Salén,[1] Vasyl Yatsyna,[2] Luca Schio,[3] Raimund Feifel,[2] Robert Richter,[4] Michele Alagia,[3] Stefano Stranges,[3,5] and Vitali Zhaunerchyk[2,a)]
[1]*Department of Physics, Stockholm University, 106 91 Stockholm, Sweden*
[2]*Department of Physics, University of Gothenburg, 412 96 Gothenburg, Sweden*
[3]*IOM-CNR Tasc, SS-14, Km 163.5 Area Science Park, Basovizza, I-34149 Trieste, Italy*
[4]*Elettra - Sincrotrone Trieste, Area Science Park, 34149 Basovizza, Trieste, Italy*
[5]*Dipartimento di Chimica e Tecnologie del Farmaco, Universitá Sapienza, Roma I-00185, Italy*

(Received 29 March 2016; accepted 13 June 2016; published online 29 June 2016)

Near-edge X-ray absorption fine-structure (NEXAFS) spectra measured at the C, N, and O *K*-edges for three molecules containing the amide moiety, *N*-methylformamide ($HCONHCH_3$), *N,N*-dimethylformamide ($HCON(CH_3)_2$), and *N,N*-dimethylacetamide ($CH_3CON(CH_3)_2$) are presented. These molecules have similar structures and differ by the number of methyl groups located at the molecular ends. The fragmentation of these molecules after resonant excitation at different *K*-edge resonances is also investigated, using a 3D-ion imaging time-of-flight spectrometer. A comparison between the molecules with respect to the relative contributions of the fragments created upon excitation at distinct resonances reveals site-specific fragmentation. Further information about the character of the core-excitation and dissociation process is obtained from the angular distributions of the ion fragments. *Published by AIP Publishing.* [http://dx.doi.org/10.1063/1.4954704]

I. INTRODUCTION

Near-edge X-ray absorption fine-structure (NEXAFS) spectroscopy is an element specific technique which is very useful for molecular electronic structure determination.[1,2] In NEXAFS an X-ray photon promotes an inner-shell electron to an unoccupied molecular orbital forming a core excited state. In light atom molecules such a state mainly decays by Auger emission which is usually followed by fragmentation of the molecule. The idea of selectively breaking specific bonds of a molecule by tuning the X-ray photon energy to the core-edge of a particular element is tempting due to its potential for control of chemical reactions. The expectation for such controlled photo-induced fragmentation stems from the excitation of spatially localized core electrons, and the ultrafast time scale (<10 fs) of the subsequent Auger decay. The selective bond breaking is perhaps most easily understood intuitively for resonant excitation to an anti-bonding orbital followed by spectator Auger decay, in which the excited electron stays in the populated orbital. If the anti-bonding orbital is localized one could further expect to preferentially break this bond.[3,4] Many experimental studies have been devoted to the investigation of site-selective bond breaking induced by core excitation both in the gas-phase[5–15] and on solid surfaces,[4,16–18] and it has been demonstrated in both cases. Due to the high cross-section[4] and the potential anti-bonding character of the populated orbital, resonant excitation is expected to be more promising for selective fragmentation compared with core-ionization, although selectivity has also been observed in the latter case.[19–27]

Amino acids and peptides have previously been investigated with NEXAFS spectroscopy.[14,28–48] Those studies revealed similarities, like the tendency that the NEXAFS spectra at the C, N, and O *K*-edges contain a strong peak typically located at about 288 eV, 402 eV, and 532 eV, respectively. These peaks were assigned to core electron excitation from the CON moiety to the Lowest Unoccupied Molecular Orbital (LUMO) of π^* character. Site-specific fragmentation of molecules containing the peptide bond have also been studied. In particular, we previously investigated the selectivity in the fragmentation of *N*-methylacetamide, $CH_3CONHCH_3$, upon excitation of different C, N, and O *K*-edge pre-edge resonances, and selective formation of specific fragments was demonstrated.[11] For example, the selective cleavage of the bonds connected with the N atom was observed upon excitation of the strongest N 1*s* resonance, although the site-selective dissociation channels were not dominant compared with other channels. Moreover, stronger tendencies towards selective bond breaking were found monitoring singly charged, compared with doubly charged, parent ion decay processes.

In this paper we present NEXAFS spectra measured at the C, N, and O *K*-edges of simple organic molecules of similar structure with increasing complexity, namely, *N*-methylformamide (MF), $HCONHCH_3$, *N,N*-dimethylformamide (DMF), $HCON(CH_3)_2$, and *N,N*-dimethylacetamide (DMA), $CH_3CON(CH_3)_2$. We also investigate the relative contribution of specific dissociation ion products associated with the excitation of different

a)Electronic mail: vitali.zhaunerchyk@physics.gu.se

pre-edge resonances. The aim is to obtain deeper insight into the possibility of site-specific fragmentation, and to find similarities in fragmentation patterns between different molecules upon exciting similar pre-edge resonances. MF is of particular interest for bio-chemistry as it contains a peptide bond, C(=O)—NH, and can serve as a simple peptide model molecule. In both DMF and DMA the hydrogen atom of the peptide link is substituted with a methyl group, while the amide moiety, on which the π^* orbital responsible for the strongest NEXAFS features in peptides is located, stays intact.

II. EXPERIMENTAL DESCRIPTION

The experiment was performed at the gas-phase undulator beam line of the Elettra synchrotron radiation facility[49] in Trieste, Italy, which provides 100% linearly polarized light. The photon energy was set by the undulator gap and the monochromator which provided a spectral resolution of ≈40, 50, and 100 meV for acquisition of high resolution NEXAFS at the C, N, and O K-edges, respectively. The samples of MF, DMF, and DMA were obtained commercially with a purity of ≥99%. An effusive molecular beam source allowed the sample to enter the interaction region where it was crossed with the X-ray beam. The created charged fragments were detected in coincidence using a position sensitive time-of-flight (TOF) imaging detector[50,51] which permitted measuring the momentum of all ions. The detector axis was oriented perpendicular to the polarization and propagation axes of the radiation, and the achieved ion detection efficiency was estimated to be ≈36% using the method described in Ref. 11. The ion TOF clock was triggered by the signal generated from the electrons emitted in the ionization region, which were collected with a MCP detector located opposite to the ion TOF spectrometer.[50,51] The NEXAFS spectra were also obtained by measuring the yield of the emitted electrons. During the NEXAFS scan a photodiode monitored the variation in X-ray intensity as a function of photon energy which was needed for normalisation of the spectra. The NEXAFS spectra were calibrated using CO_2[52] and N_2[53] data as known reference cases.

The below-resonance (BR) contribution measured at the photon energies of 270 eV and 280 eV for MF and DMF/DMA, respectively, was subtracted from the mass spectra recorded on resonance, unless otherwise stated. To properly subtract the non-resonant contributions, the mass spectra were normalized to the intensity of the Ar^{2+} peak at $m/z = 20$ which guarantees equivalent total photon flux. The Ar gas was admitted to a section of the beam line located upstream with respect to the detector chamber and intercepted by the incidence beam. The single-ion mass spectra have been corrected for false contributions from double, triple, and quadruple fragmentation channels where a part of the ions is not detected due to the partial (36%) detection efficiency. All presented spectra have been binned by $m/z = 0.05$. A NEXAFS scan was recorded before each mass spectrum acquisition in order to correctly set the desired photon energy.

MF mass spectra were additionally measured with the position sensitive detector replaced by a fast single anode microchannel plate detector.

III. RESULTS AND DISCUSSION

A. NEXAFS spectra

Experimental NEXAFS spectra for MF, DMF, and DMA are presented in Fig. 1, where the (a), (b), and (c) subplots show the spectra measured at the C, N, and O K-edges, respectively. The NEXAFS spectra of MF have recently been investigated, both experimentally and theoretically.[14] The MF spectra of Fig. 1, obtained with higher statistics and resolution, agree with the previously published ones. The spectral assignments given in the previous work[14] point out that the main MF NEXAFS structures at 288.0 eV, 401.9 eV, and 531.9 eV are associated with excitation of the core-electrons from the C, N, and O atoms, respectively, from the peptide moiety, to a π^* orbital which has a strong C—O and C—N anti-bonding character ($\pi^*_{C=O}\pi^*_{C-N}$).

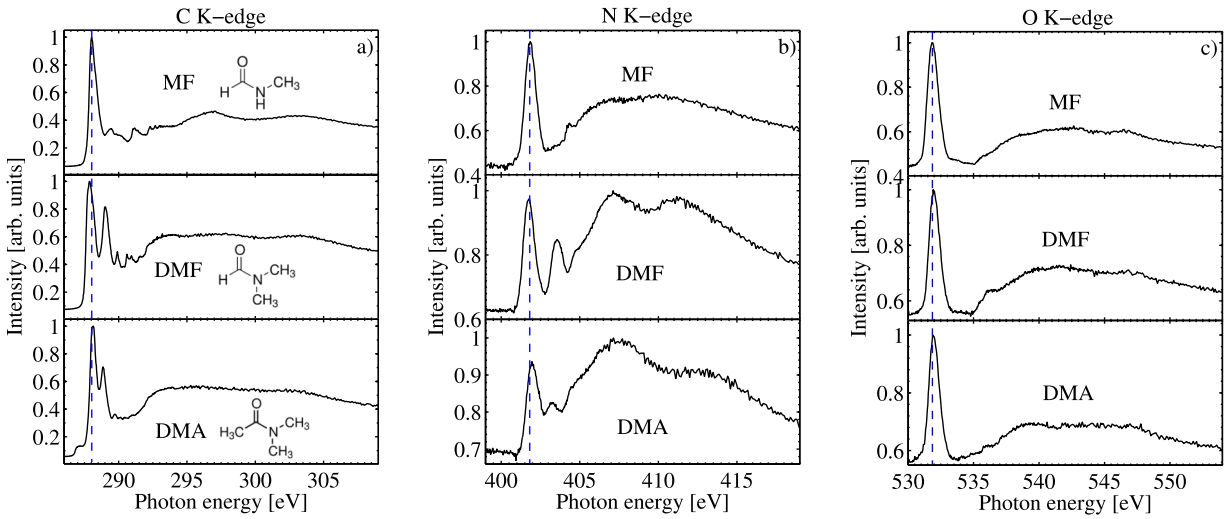

FIG. 1. NEXAFS spectra: ((a)-(c)) present the spectra measured at the C, N, and O K-edges, respectively. The MF, DMF, and DMA data are shown in the top, middle, and bottom panels, respectively. The dashed blue lines point at the photon energy axis to the positions of the strongest MF peaks at 288.0 eV (a), 401.9 eV (b), and 531.9 eV (c).

The O 1*s* NEXAFS spectra for the three molecules (Fig. 1(c)) are very similar, i.e., they consist of one strong peak located at ≈532.0 eV (531.9 eV, 532.0 eV, and 532.0 eV for MF, DMF, and DMA, respectively). Such a similarity can be understood by considering that the molecules contain only one oxygen atom located in similar chemical environments as a part of the carbonyl group. The C 1*s* and N 1*s* NEXAFS spectra are also similar in the sense that their strongest peaks have nearly equal positions: 288.0 eV (MF), 287.8 eV (DMF), and 288.1 eV (DMA) at the C *K*-edge (Fig. 1(a)); and 401.9 eV (MF), 401.7 eV (DMF), and 402.1 eV (DMA) at the N *K*-edge (Fig. 1(b)). To the best of our knowledge, assignments of the peaks in the DMF and DMA NEXAFS spectra based on quantum chemical calculations are not yet available. However, the similarities in the positions of the strongest peaks in the NEXAFS spectra at each edge might suggest that they are associated with similar transitions. If this is indeed the case, then the results of the calculations carried out for MF[14] can be extended to DMF and DMA implying that the strongest NEXAFS features in the DMF and DMA spectra are due to the core-electron transitions from the CON moiety to a π^* orbital of anti-bonding character along the C—O and N—C bonds. Such an interpretation is further supported by the fact that the molecules have similar structures, differing only by additional methyl groups located at the molecular ends while the CON moiety stays intact.

The DMF C 1*s* and N 1*s* NEXAFS spectra (the middle panels in Figs. 1(a) and 1(b)) contain additional relatively intense features at higher excitation energies, which are located at 289.0 eV and 403.6 eV, respectively. Additional peaks are also observed for DMA at 288.9 eV and 403.2 eV (the bottom panels in Figs. 1(a) and 1(b)), although they are weaker compared with the case of DMF. Previous NEXAFS studies of MF and NMA (*N*-methylacetamide)[14] suggest that in the case of the N *K*-edge spectra, the extra feature at higher energy in DMF and DMA is due to N 1*s* electron excitations into empty MOs of diffuse Rydberg character. In the C *K*-edge spectra of DMF and DMA, the extra peaks at higher energies are attributed, as suggested by the previous theoretical NEXAFS studies,[14,54] to C 1*s* transitions from the carbon atoms of the methyl groups to unoccupied diffuse Rydberg orbitals. The weak structure just below the main peak of DMA is also observed in NMA.[11,54] These two molecules, unlike MF and DMF, have a methyl group attached to CO. Indeed, as was verified theoretically for NMA in Ref. 54, the low energy peak C *K*-edge NEXAFS peak is associated with C 1*s* excitation from the methyl group of the CH_3CO moiety.

B. Angular distribution

Additional information on the character of the core-excitation transitions can be derived from analysis of the spatial product distributions. In the general case the product distributions, $P(\phi)$, can be described as

$$P(\phi)/\sin\phi \propto 1 + \frac{\beta}{2}\left(3\cos^2\phi - 1\right), \qquad (1)$$

where ϕ is the angle between the product momentum and the light polarization axis, β is the asymmetry parameter which ranges between −1 and 2, and relates to the character of the transition as well as the molecular fragmentation dynamics. The imaging detector utilized in the present study enables measuring spatial distributions of ion products. In particular, since a multi-anode detector plate and multistop electronics are used, all ion momentum vectors can be determined.

In the angular distribution analysis, we concentrate on DMF for which the NEXAFS spectra have not been assigned and for which, unlike DMA, suitable two-body channels from doubly charged parent ions were available for an accurate determination of β. Despite that the production of singly charged parent ions dominate over dications, we have chosen the $HCO^+ + N(CH_3)_2^+$ dissociation channel for the analysis because this channel consists of two charged products, the total mass of which is equal to the parent molecule mass, i.e., this channel does not involve formation of any neutral fragment. This implies that complete momenta of the HCO^+ and $N(CH_3)_2^+$ fragments can accurately be obtained which is a prerequisite for accurate determination of product spatial distributions. In this channel the C(O)—N bond is broken, and if the core-excitation is governed by a perpendicular dipole moment transition with respect to this bond and if the fragmentation occurs promptly after the photon absorption and the subsequent Auger decay, the fragments will be ejected orthogonally with respect to the light polarization and the angular distribution is described by Eq. (1) with $\beta = -1$. For the core-excitation governed by a parallel dipole moment transition followed by prompt Auger decay and molecular fragmentation, the fragments are ejected parallel to the light polarization and the angular distribution is described by Eq. (1) with $\beta = 2$. If the fragmentation is not prompt with respect to the excitation, the angular distribution will tend to be more isotropic and the fully isotropic distribution is presented by Eq. (1) with $\beta = 0$.

Figure 2 shows the angular distributions of the ion fragments detected in coincidence originating from the $HCON(CH_3)_2^{2+} \rightarrow HCO^+ + N(CH_3)_2^+$ dissociation channel at

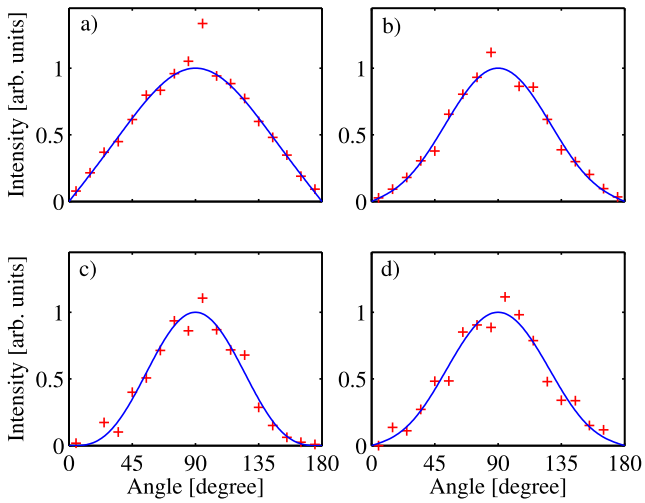

FIG. 2. Angular distribution of the HCO^+ and $N(CH_3)_2^+$ ions when DMF was excited with the photon energies of (a) 280 eV (BR), (b) 287.8 eV (C 1*s*), (c) 401.7 eV (N 1*s*), and (d) 532.0 eV (O 1*s*). The blue curves are described by Eq. (1).

several excitation energies. The angular distributions have been subtracted by the BR contribution and thus represent the distributions associated solely with the K-shell resonances. Table II lists β parameters obtained by least squared fitting of the experimental angular distributions with Eq. (1). The β parameter obtained for the strongest N 1s NEXAFS peak at 401.7 eV is −1.0, which means that the fragments are ejected orthogonally to the X-ray polarization direction. This is what would be expected for a $1s \rightarrow \pi^*$ transition if assuming an instantaneous break-up. A higher $\beta = -0.64$ and −0.74, obtained for the strongest C 1s and O 1s NEXAFS peaks, respectively, suggests that if these excitations are associated with the C and O $1s \rightarrow \pi^*$ transitions, then molecular break-up does not occur instantaneously with respect to the X-ray photon absorption. We note that the assignment of the strongest DMF NEXAFS features at the C, N, and O K-edges to the orbital of π^* character is in line with the argumentation given in Sec. III A.

The β values of the additional peaks located at 289.0 eV and 403.6 eV are −0.37 and −0.76, respectively. They exhibit a similar increase of ~0.25 relative to the largely negative β of their respective main peak. The different β values measured at higher energies in the C 1s and N 1s NEXAFS spectra of DMF can be due to different orientations of the transition moment vectors of the involved excitation processes with respect to the broken peptide bond. The β values can also be affected by the decay dynamics of different dissociation mechanisms contributing to the selected ion-ion channel ($HCO^+ + N(CH_3)_2^+$), i.e., a number of molecular states can be populated after the Auger decay and the angular distribution measured then represents a superposition of angular distributions associated with various molecular states.

C. Fragmentation patterns

Here we focus on the mass spectra of single ions, because the fragmentation of singly charged parent ions after K-shell excitation has shown more site-specificity[11,56] when compared to that of multiply charged ones. Furthermore, singly charged parent ions are expected to dominate over other charge states in ion spectra recorded at resonance photon energies.

Figure 3 displays the mass spectra at the most intense NEXAFS resonances (Fig. 1) of MF (a), DMF (b), and DMA (c) associated with the decay of singly charged parent ions, and Tables I–III list the corresponding relative ion yields. Tables I–III for the three molecules reveal that the singly charged ion production is characterized by a relatively high parent ion contribution at BR photon energies, namely at $m/z = 59$, 73, and 87, respectively, for MF, DMF, and DMA, whilst it becomes negligible at resonance energies. The parent ion production for MF and DMF is very close to the one measured in the VUV energy regime at 20 eV,[55] where valence photoionization exclusively yields singly charged ions. The 20 eV and 270/280 eV mass spectra are generally similar (Tables I and II), despite the additional dissociation channels such as inner valence, double- and multiple-electron ionization-excitation processes accessible at the higher excitation energies of 270/280 eV.

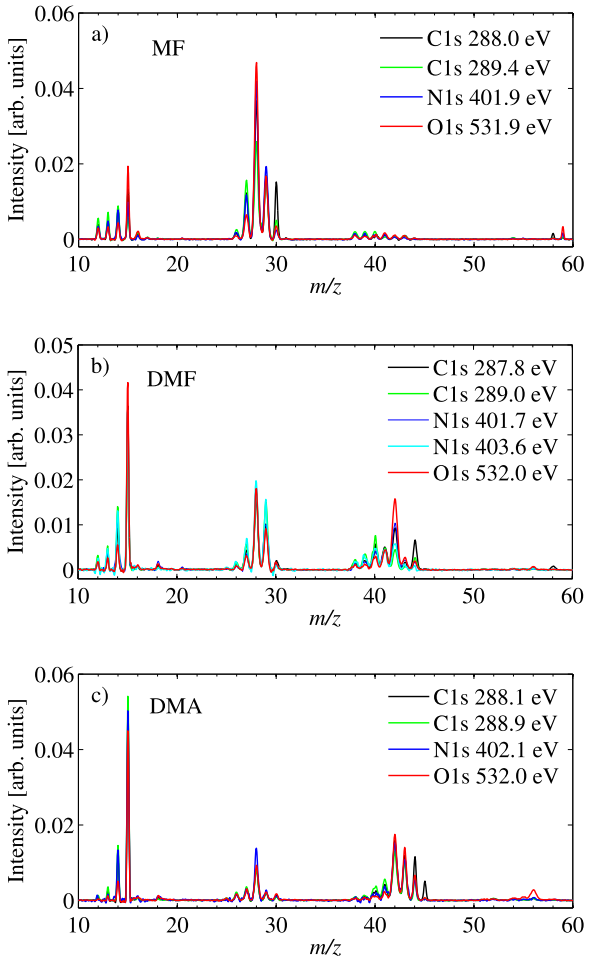

FIG. 3. ((a)–(c)) Single-ion mass spectra of MF, DMF, and DMA, respectively, for different K-shell electron excitation energies. Each spectrum is normalized to its integrated intensity in order to elucidate the spectral differences. In the spectra, the peaks of argon at $m/z = 13.3$, 20, and 40, which were used for BR spectrum normalization purposes, have been removed.

From Fig. 3 one may observe that upon excitation of the strongest C K-edge resonance (the black curves) all three molecules display an enhanced probability (compared with the other resonances) of breaking the bonds of the CON moiety, and produce fragments which are intact on the N-side of the C(O)—N bond. For MF, DMF, and DMA this leads to formation of the $NHCH_3^+$ ($m/z = 30$), $N(CH_3)_2^+$ ($m/z = 44$), and $N(CH_3)_2^+$ ($m/z = 44$) fragments, respectively. Moreover, in the case of DMA the $NH(CH_3)_2^+$ ion ($m/z = 45$) production, which involves the C(O)—N bond breaking accompanied by molecular re-arrangement, is almost exclusively produced at this C 1s resonance. Such a tendency supports again the assertion that the molecular orbitals associated with the strongest K-shell resonance in the three molecules have similar characters. It also suggests site-specificity of bond rupture, as one could expect from K-shell excitation of the carbon atom located at the CON moiety to a π^* orbital with C—N and C—O anti-bonding character. We note from Tables I–III that BR excitation produces higher relative yields of the above mentioned ions ($m/z = 30$, 44, 44, respectively) than the C $1s \rightarrow \pi^*$ resonance. This represents the different process of valence ionization which does not involve resonant excitation

TABLE I. Relative single-ion yields (%) of MF at different photon excitation energies. The data at 20 eV are adopted from Ref. 55 for direct comparison. A roughly estimated probability of peptide-bond breaking (pbb) is listed in the bottom row.

			C 1*s*			
		BR			N 1*s*	O 1*s*
m/*z*	20 eV	270 eV	288.0 eV	289.4 eV	401.9 eV	531.9 eV
1	…	5	10	13	11	4
2	…	0	1	1	1	0
12	…	1	2	3	2	2
14	…	3	4	5	5	2
15	8	5	7	3	5	9
16	…	1	1	1	0	3
17	1	0	0	0	0	0
18	4	2	0	0	0	0
26	…	0	1	2	2	1
27	…	6	10	14	10	7
28	24	30	33	25	38	45
29	7	14	14	16	18	14
30	40	16	9	3	2	2
31	1	0	0	0	0	0
38	…	0	1	2	1	1
39	…	1	1	2	1	1
41	0	1	1	1	1	2
44	0	0	0	0	0	0
58	2	1	1	0	0	0
59	13	14	0	0	1	2
pbb		55	55	49	59	52

TABLE II. Relative single-ion yields (%) and β values of DMF at different photon excitation energies. The β values were obtained for the $HCON(CH_3)_2^{2+} \rightarrow HCO^+ + N(CH_3)_2^+$ channel. The data at 20 eV are adopted from Ref. 55 for direct comparison.

			C 1*s*		N 1*s*		
		BR					O 1*s*
m/*z*	20 eV	280 eV	287.8 eV	289.0 eV	401.7 eV	403.6 eV	532.0 eV
1	…	3	5	8	6	7	4
2	…	0	1	1	1	1	1
12	…	1	1	2	1	1	1
14	…	2	5	8	8	7	3
15	3	13	19	16	18	20	20
16	0	1	1	1	1	1	1
17	1	1	0	0	0	0	0
18	9	3	1	0	1	0	1
19	0	1	0	0	0	0	0
25	0	0	0	0	0	1	0
26	0	0	1	2	1	2	1
27	2	2	4	5	3	6	3
28	8	13	15	16	17	19	16
29	2	8	10	14	12	14	8
30	10	3	1	1	1	1	1
31	1	0	0	0	0	0	0
38	…	1	2	3	1	2	1
39	…	1	3	4	3	4	2
41	0	4	7	6	6	5	5
42	13	13	11	5	14	8	20
43	4	3	2	1	3	1	4
44	30	11	6	3	2	1	2
45	1	0	0	0	0	0	0
56	1	0	0	0	0	0	1
58	1	1	1	0	0	0	0
72	1	1	1	0	0	0	0
73	13	12	0	0	1	0	2
74	1	0	0	0	0	0	0
β	…	−0.17	−0.64	−0.37	−1.00	−0.76	−0.74

from a localized core hole and, as discussed further below, the high yield in this case is related to the tendency of statistical fragmentation to break the weak bonds, such as the peptide-bond. It also follows from Fig. 3 that the intensity of the $HCNH^+$ (m/z = 28), $HCNCH_3^+$ (m/z = 42), and $CH_3CNCH_3^+$ (m/z = 56) products is enhanced for MF, DMF, and DMA, respectively, when the main O 1*s* resonance is excited. For the three molecules, production of these fragments is associated with the detachment of the oxygen atom and one methyl group. As was discussed above, the main O 1*s* resonance is associated with the excitation of an electron from the O 1*s* orbital of the carbonyl group to the π^* orbital which has an anti-bonding character along the carbonyl bond. This observation provides another indication of site-specific fragmentation where the bond rupture occurs around the site on which the *K*-shell electron is excited.

MF is the simplest model of a peptide, and Lin *et al.*[14] concluded that the lowest core-electron excitation preferentially (with the probability of 59%-71% for the C, N, and O *K*-edges) leads to the cleavage of the peptide bond. This was explained by the nature of the orbital which is strongly anti-bonding at the peptide bond. For comparison, a corresponding estimate of the probability for breaking the peptide bond was performed from our MF single-ions data. Here the relative yields of the fragments with m/z = 26–30 were added and corrected for the fraction of fragments not associated with breaking of the peptide bond, as given in Ref. 14 for the C, N, and O 1s → π^* excitations. Applying the same correction for all three excitations around the C *K*-edge allowed an estimate of the peptide-bond-breaking probabilities for the different transitions, as presented in Table I (pbb). We obtain probabilities of 55% for both 270 eV (BR) and 288.0 eV (C 1s → π^*) excitation (Fig. 1). Although Lin *et al.*[14] did not report this value for BR, for the C 1*s* → π^* excitation our value of 55% agrees well with their finding of 59%. From our results, it appears that the weak peptide bond is as likely to break for the BR excitation as for the C 1*s* → π^* resonance excitation. A high probability of breaking of the peptide bond is a known and well studied phenomenon when peptide fragmentation is activated with black-body radiation,[57] infrared multi-photon excitation,[58] ultraviolet[59] and vacuum ultraviolet[60] excitation, and collisions with gas-phase molecules or surfaces.[61,62] The above studies use moderate excitation energies and our results suggest that the propensity to break the peptide bond seems to be preserved even for larger excitation energies. We thus conclude that the C 1s → π^* resonance excitation is not uniquely responsible for highly selective dissociation of the peptide bond. However, the influence from its anti-bonding character is observed by investigating the relative yields of individual masses, when compared to other resonances, i.e., not comparing with the BR excitation, as discussed above.

TABLE III. Relative single-ion yields (%) of DMA at different photon excitation energies.

		C 1*s*			
m/*z*	BR 280 eV	288.1 eV	288.9 eV	N 1*s* 402.1 eV	O 1*s* 532.0 eV
1	1	3	4	4	1
2	0	0	1	0	1
7	0	1	1	1	1
12	0	0	1	0	0
14	2	5	7	7	2
15	15	23	26	24	20
16	1	1	1	1	1
18	2	1	0	1	1
19	1	0	0	0	1
25	0	0	1	0	0
26	0	1	2	1	1
27	1	2	3	3	2
28	6	7	7	11	8
29	1	2	2	2	2
30	2	1	1	1	2
38	0	1	1	1	1
39	0	1	2	1	1
41	3	5	7	4	3
42	15	17	15	18	19
43	15	11	10	12	13
44	15	8	4	4	5
45	3	3	0	0	1
52	0	1	1	0	1
53	0	0	0	0	0
54	0	1	0	0	1
55	0	0	0	0	1
56	1	1	1	1	4
57	0	0	0	0	1
58	1	0	0	0	1
72	2	1	0	0	1
87	10	0	0	1	1

Furthermore, the anti-bonding character manifests itself in the estimated probability of peptide-bond breaking, which for the two resonances at the C *K*-edge is approximately 10% higher at the 288 eV (C 1s $\rightarrow \pi^*$) resonance than at the 289.4 eV resonance, as presented in Table I (pbb).

D. Fragmentation of doubly charged ions

Figure 4 shows the ion-ion coincidence map of MF recorded at 288.0 eV, which corresponds to the main C $1s \rightarrow \pi^*$ resonance. The figure displays several groups of coincidence islands (groups A-D), and horizontal and vertical lines which originate from accidental coincidence events. Three groups of coincidence islands correlate with m/z = 12–15 and represent predominantly CH_x^+ (x = 0–3) detected in coincidence with other fragments (groups A-C). If the probability for molecular rearrangement is negligibly small, group C represents the detachment of the methyl moiety with the peptide bond in the remaining fragment being intact. A group of coincidence islands may also be observed at m/z = 27–30 on both axes (group D). The correlations of group D represent the fragmentation of doubly charged ions where the peptide bond is broken, together with the loss of

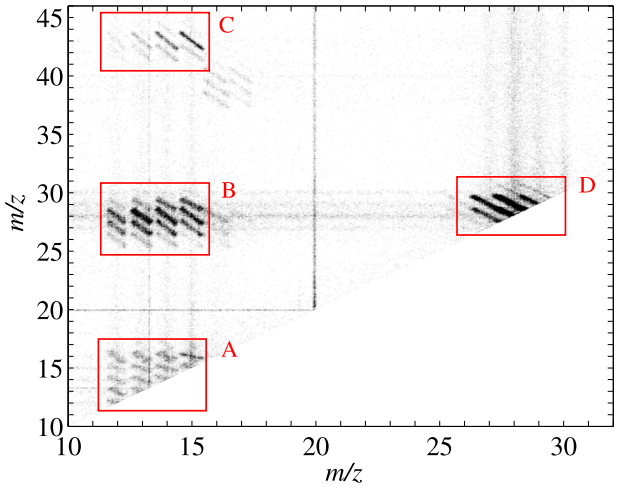

FIG. 4. Coincidence map for the C $1s \rightarrow \pi^*$ excitation (288.0 eV) of MF. The BR contribution has not been removed.

one or more H-atoms. Fragmentation associated with rupture of the peptide bond is also represented by the coincidences in group A if the correlations with m/z = 16 are excluded. Since group B consists of the islands associated both with the intact peptide bond and peptide-bond rupture, we use the sum of the main coincidence islands of group A (excluding m/z = 16) and D, divided by the added contribution of the most significant correlations of the whole map, to estimate the probability for cleavage of the peptide bond. This is displayed in the top row of Table IV for distinct resonances of MF, where the values have been normalized to that of BR (0.58). It shows again a large contribution of peptide-bond breakage at BR excitation. In contrast to the case of fragmentation of singly charged ions, the peptide-bond cleavage is not enhanced at the C $1s \rightarrow \pi^*$ excitation compared with the higher lying resonance (289.4 eV) of the C *K*-edge. The difference observed between single-ions (Table I (pbb)) and ion-pairs (Table IV (top row)) is related to the difference in fragment yields. Figure 5 compares the partial ion-yield (PIY) curves of single ions (solid line) and ion-pairs (dashed line) of MF for m/z = 26–30 as a function of photon energy at the C *K*-edge. It reveals a particularly large difference in PIY between the single ions and ion-pairs for m/z = 30, for which the ion-pair contribution is almost negligible throughout the photon energy range. The markedly different response of parent ions with one or two charges underlines the importance of their separate analysis.

TABLE IV. Relative significance of dissociation associated with cleavage of the peptide bond (first row), and with the detachment of O or OH (second, third row, respectively), from doubly charged MF parent ions. The values of all rows are normalized to the BR contribution. BR contributions have been subtracted for all data corresponding to non-BR excitation.

		C 1*s*			
Ion pairs (*m*/*z*)	BR 270 eV	288.0 eV	289.4 eV	N 1*s* 401.9 eV	O 1*s* 531.9 eV
A and D regions	1	0.85	0.98	0.86	0.65
16 (O) & all	1	1.17	0.93	1.35	1.70
17 (OH) & all	1	1.29	0.80	0.96	1.32

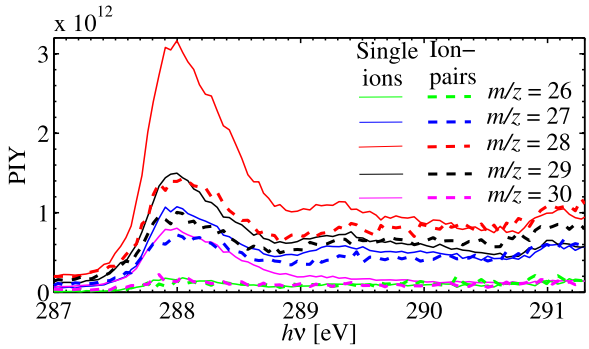

FIG. 5. PIY for $m/z = 26$–30 as a function of photon energy at the C K-edge for MF. The solid and dashed lines represent PIYs from single ions and ion-pairs, respectively. The BR contribution has not been removed.

Figure 4 also displays coincidence islands that correlate with $m/z = 16$ (O) and 17 (OH). Table IV shows the relative intensities of the O^+ and OH^+ fragments obtained from ion pairs. It reveals a pronounced increase of O^+ detachment at the O 1s resonance excitation. This supports a site-specific bond rupture of the O-atom, as discussed above for singly charged parent ions, also for the doubly charged case. Moreover, one observes a significantly higher yield of OH^+ fragments at the C 1s 288.0 eV and O 1s resonance excitations. For the O 1s resonance it is a consequence of the increased probability for O^+ detachment. The C 1s 288.0 eV resonance is associated with a $1s \rightarrow \pi^*$ excitation where the 1s electron resides on the carbon atom of the H—C—O group. Thus the higher yield of OH^+ fragments suggests that this ion is formed by the H-atom of the H—C—O group connecting with the O^+ ion.

IV. CONCLUSIONS

The fragmentation of MF, DMF, and DMA upon resonant K-edge excitation has been investigated by means of NEXAFS and ion TOF mass spectrometry. These molecules exhibit strong structural similarities as they all contain the amide moiety and only differ by the number of methyl groups. This allows for the study of common features upon resonant K-shell electron excitations, associated with certain molecular structures. In particular we have investigated the site-specificity of fragmentation for these molecules by comparison of the fragment yields at several resonant C 1s, N 1s, and O 1s excitations. The results for the different molecules display similarities which confirm tendencies towards the preferential breaking of specific bonds upon excitation at particular inner-shell pre-edge resonances. Our measurements also confirm the findings of Lin *et al.*[14] of a high probability for cleavage of the peptide bond (≈55%) after K-shell excitation. However, from our results this high probability appears to be a general feature of the peptide-model systems which is not necessarily associated with resonant K-shell excitation but is also observed in valence ionization. Still, in comparison with different K-edge pre-edge resonances, increased fragmentation associated with peptide-bond rupture can be observed for specific transitions. We also demonstrate pronounced differences between singly and doubly charged parent ions in the probability of peptide-bond cleavage with respect to the excited resonance.

Moreover, angular distributions of ionic products formed after the K-shell excitation have been analyzed in the case of DMF for the specific dication dissociation channel yielding HCO^+ and $N(CH_3)_2^+$ fragments. The obtained results support previous assignments of the dominant NEXAFS feature for similar amide systems as the $1s \rightarrow \pi^*$ transition involving an atomic core hole located at the OCN moiety. Furthermore, the β values obtained from the ion angular distributions of the selected dication dissociation channel suggest a longer fragmentation time following the C $1s \rightarrow \pi^*$ and O $1s \rightarrow \pi^*$ transitions, compared with the corresponding N 1s transition.

ACKNOWLEDGMENTS

This work has been financially supported by the Swedish Research Council (VR) and the Knut and Alice Wallenberg Foundation, Sweden. P.S. acknowledges support from the Stockholm-Uppsala Centre for Free Electron Laser Research (SUFEL). V.Y. acknowledges Paul och Marie Berghaus donationsfond for the financial support for traveling. L.S. thanks the CNR-IOM Institute for financial support under the EUROFEL Design Study Project. The authors also acknowledge the open access contribution of the Research Infrastructure (RI) Elettra.

[1]J. Stöhr, in *NEXAFS Spectroscopy*, edited by G. Erti, R. Gomer, and D. L. Mills, Springer Series in Surface Sciences (Springer-Verlag, Berlin, Heildelberg, New York, 1992), Vol. 25.
[2]G. Hähner, Chem. Soc. Rev. **35**, 1244 (2006).
[3]M. C. K. Tinone, K. Tanaka, J. Maruyama, N. Ueno, M. Imamura, and N. Matsubayashi, J. Chem. Phys. **100**, 5988 (1994).
[4]Y. Baba, Low Temp. Phys. **29**, 228 (2003).
[5]X. J. Liu, G. Prümper, E. Kukk, R. Sankari, M. Hoshino, C. Makochekanwa, M. Kitajima, H. Tanaka, H. Yoshida, Y. Tamenori, and K. Ueda, Phys. Rev. A **72**, 042704 (2005).
[6]A. Naves de Brito, R. Feifel, A. Mocellin, A. B. Machado, S. Sundin, I. Hjelte, S. L. Sorensen, and O. Björneholm, Chem. Phys. Lett. **309**, 377 (1999).
[7]A. Naves de Brito, S. Sundin, R. R. Marinho, I. Hjelte, G. Fraguas, T. Gejo, N. Kosugi, S. Sorensen, and O. Björneholm, Chem. Phys. Lett. **328**, 177 (2000).
[8]K. Ueda, M. Simon, C. Miron, N. Leclercq, R. Guillemin, P. Morin, and S. Tanaka, Phys. Rev. Lett. **83**, 3800 (1999).
[9]P. Erman, A. Karawajczyk, E. Rachlew, M. Stankiewicz, and K. Y. Franzen, J. Chem. Phys. **107**, 10827 (1997).
[10]P. Morin, M. Simon, C. Miron, N. Leclercq, E. Kukk, J. D. Bozek, and N. Berrah, Phys. Rev. A **61**, 050701 (2000).
[11]P. Salén *et al.*, Phys. Chem. Chem. Phys. **16**, 15231 (2014).
[12]Y.-S. Lin, S.-Y. Lin, Y. T. Lee, C.-M. Tseng, C.-K. Ni, C.-L. Liu, C.-C. Tsai, J.-L. Chen, and W.-P. Hu, J. Phys. Chem. A **118**, 7803 (2014).
[13]Y.-S. Lin, K.-T. Lu, Y. T. Lee, C.-M. Tseng, C.-K. Ni, and C.-L. Liu, J. Phys. Chem. A **118**, 1601 (2014).
[14]Y.-S. Lin *et al.*, J. Phys. Chem. A **119**, 6195 (2015).
[15]M. Sakai, K. Okada, K. Ohnoa, and K. Tabayashia, J. Mass Spectrom. **45**, 306 (2010).
[16]S. Wada, H. Kizaki, Y. Matsumoto, R. Sumii, and K. Tanaka, J. Phys.: Condens. Matter **18**, S1629 (2006).
[17]E. Ikenaga, K. Kudara, K. Kusaba, K. Isari, S. A. Sardar, S. Wada, K. Mase, T. Sekitani, and K. Tanaka, J. Electron Spectrosc. Relat. Phenom. **114–116**, 585 (2001).
[18]E. O. Sako, Y. Kanameda, E. Ikenaga, M. Mitani, O. Takahashi, K. Saito, S. Iwata, S. Wada, T. Sekitani, and K. Tanaka, J. Electron Spectrosc. Relat. Phenom. **114–116**, 591 (2001).
[19]J. H. D. Eland, P. Linusson, M. Mucke, and R. Feifel, Chem. Phys. Lett. **548**, 90 (2012).

[20]H. Iwayama, N. Sisourat, P. Lablanquie, F. Penent, J. Palaudoux, L. Andric, J. H. D. Eland, K. Bucar, M. Zitnik, Y. Velkov, Y. Hikosaka, M. Nakano, and E. Shigemasa, J. Chem. Phys. **138**, 024306 (2013).
[21]S. Nagaoka, H. Fukuzawa, G. Prümper, M. Takemoto, O. Takahashi, K. Yamaguchi, T. Kakiuchi, K. Tabayashi, I. H. Suzuki, J. R. Harries, Y. Tamenori, and K. Ueda, J. Phys. Chem. A **115**, 8822 (2011).
[22]S. Nagaoka, G. Prümper, H. Fukuzawa, M. Hino, M. Takemoto, Y. Tamenori, J. Harries, I. H. Suzuki, O. Takahashi, K. Okada, K. Tabayashi, X.-J. Liu, T. Lischke, and K. Ueda, Phys. Rev. A **75**, 020502 (2007).
[23]K. Le Guen, M. Ahmad, D. Ceolin, P. Lablanquie, C. Miron, F. Penent, P. Morin, and M. Simon, J. Chem. Phys. **123**, 084302 (2005).
[24]C. Miron, M. Simon, N. Leclercq, D. L. Hansen, and P. Morin, Phys. Rev. Lett. **81**, 4104 (1998).
[25]A. Mocellin, K. Wiesner, S. L. Sorensen, C. Miron, K. Le Guen, D. Céolin, M. Simon, P. Morin, A. B. Machado, O. Björneholm, and A. Naves de Brito, Chem. Phys. Lett. **435**, 214 (2007).
[26]H. Fukuzawa, G. Pruemper, X.-J. Liu, E. Kukk, R. Sankari, M. Hoshino, H. Tanaka, Y. Tamenori, and K. Ueda, Chem. Phys. Lett. **436**, 51 (2007).
[27]E. Itälä, D. T. Ha, K. Kooser, M. A. Huels, E. Rachlew, E. Nmmiste, U. Joost, and E. Kukk, J. Electron Spectrosc. Relat. Phenom. **184**, 119 (2011).
[28]Y. Zubavichus, O. Fuchs, L. Weinhardt, C. Heske, E. Umbach, J. D. Denlinger, and M. Grunze, Radiat. Res. **161**, 346 (2004).
[29]Y. Zubavichus, M. Zharnikov, A. Shaporenko, and M. Grunze, J. Electron Spectrosc. Relat. Phenom. **134**, 25 (2004).
[30]Y. Zubavichus, A. Shaporenko, M. Grunze, and M. Zharnikov, J. Phys. Chem. B **111**, 9803 (2007).
[31]Y. Zubavichus, A. Shaporenko, M. Grunze, and M. Zharnikov, J. Phys. Chem. A **109**, 6998 (2005).
[32]Y. Zubavichus, A. Shaporenko, M. Grunze, and M. Zharnikov, Nucl. Instrum. Methods Phys. Res., Sect. A **603**, 114 (2009).
[33]J. Stewart-Ornstein, A. P. Hitchcock, P. Hernández Cruz, P. Henklein, J. Overhage, K. Hilpert, J. D. Hale, and R. E. Hancock, J. Phys. Chem. B **111**, 7691 (2007).
[34]W. Zhang, V. Carravetta, O. Plekan, V. Feyer, R. Richter, M. Coreno, and K. C. Prince, J. Chem. Phys. **131**, 035103 (2009).
[35]G. Cooper, M. Gordon, D. Tulumello, C. Turci, K. Kaznatcheev, and A. P. Hitchcock, J. Electron Spectrosc. Relat. Phenom. **137**, 795 (2004).
[36]V. Feyer, O. Plekan, R. Richter, M. Coreno, K. C. Prince, and V. Carravetta, J. Phys. Chem. A **112**, 7806 (2008).
[37]H. Legall, H. Stiel, M. Beck, D. Leupold, W. I. Gruszecki, and H. Lokstein, J. Biochem. Biophys. Methods **70**, 369 (2007).
[38]M. W. Buckley and N. A. Besley, Chem. Phys. Lett. **501**, 540 (2011).
[39]V. Carravetta, O. Plashkevych, and H. Ågren, J. Chem. Phys. **109**, 1456 (1998).
[40]L. Yang, O. Plashkevych, O. Vahtras, V. Carravetta, and H. Ågren, J. Synchrotron Radiat. **6**, 708 (1999).
[41]I. Ishii and A. P. Hitchcock, J. Chem. Phys. **87**, 830 (1987).
[42]K. Kaznacheyev, A. Osanna, C. Jacobsen, O. Plashkevych, O. Vahtras, H. Ågren, V. Carravetta, and A. P. Hitchock, J. Phys. Chem. A **106**, 3153 (2002).
[43]M. L. Gordon, G. Cooper, C. Morin, T. Araki, C. C. Turci, K. Kaznatcheev, and A. P. Hitchcock, J. Phys. Chem. A **107**, 6144 (2003).
[44]E. Otero and S. G. Urquhart, J. Phys. Chem. A **110**, 12121 (2006).
[45]M. Tanaka, K. Nakagawa, T. Koketsu, A. Agui, and A. Yokoya, J. Synchrotron Radiat. **8**, 1009 (2001).
[46]K. Kummer, V. N. Sivkov, D. V. Vyalikh, V. V. Maslyuk, A. Blüher, S. V. Nekipelov, T. Bredow, I. Mertig, M. Mertig, and S. L. Molodtsov, Phys. Rev. B **80**, 155433 (2009).
[47]D. Healion, H. Wang, and S. Mukamel, J. Chem. Phys. **134**, 124101 (2011).
[48]J. Boese, A. Osanna, C. Jacobsen, and J. Kirz, J. Electron Spectrosc. Relat. Phenom. **85**, 9 (1997).
[49]R. R. Blyth, R. Delaunay, M. Zitnik, J. Krempasky, R. Krempaska, J. Slezak, K. C. Prince, R. Richter, M. Vondracek, R. Camilloni, L. Avaldi, M. Coreno, G. Stefani, C. Furlani, M. de Simone, S. Stranges, and M.-Y. Adam, J. Electron Spectrosc. Relat. Phenom. **101–103**, 959 (1999).
[50]M. Lavollée, Rev. Sci. Instrum. **70**, 2968 (1999).
[51]M. Alagia *et al.*, Chem. Phys. **398**, 134 (2012).
[52]T. K. Sham, B. X. Yang, J. Kirz, and J. S. Tse, Phys. Rev. A **40**, 652 (1989).
[53]S. Fatehi, C. P. Schwartz, R. J. Saykally, and D. Prendergast, J. Chem. Phys. **132**, 094302 (2010).
[54]C. Li, P. Salén, V. Yatsyna, L. Schio, R. Feifel, R. Squibb, M. Kamińska, M. Larsson, R. Richter, M. Alagia, S. Stranges, S. Monti, V. Carravett, and V. Zhaunerchyk, Phys. Chem. Chem. Phys. **18**, 2210 (2016).
[55]S. Leach, N. Champion, H.-W. Jochims, and H. Baumgärtel, Chem. Phys. **376**, 10 (2010).
[56]P. Salén *et al.*, J. Chem. Phys. **143**, 134302 (2015).
[57]W. D. Price, P. D. Schnier, and E. R. Williams, Anal. Chem. **68**, 859 (1996).
[58]J. A. Zimmerman, C. H. Watson, and J. R. Eyler, Anal. Chem. **63**, 361 (1991).
[59]W. D. Bowers, S. S. Delbert, R. L. Hunter, and R. T. McIver, Jr., J. Am. Chem. Soc. **106**, 7288 (1984).
[60]M. S. Thompson, W. Cui, and J. P. Reilly, Angew. Chem., Int. Ed. **43**, 4791 (2004).
[61]D. F. Hunt, W. M. Bone, J. Shabanowitz, J. Rhodes, and J. M. Ballard, Anal. Chem. **53**, 1704 (1981).
[62]E. R. Williams, K. D. Henry, F. W. McLafferty, J. Shabanowitz, and D. F. Hunt, J. Am. Soc. Mass Spectrom. **1**, 413 (1990).